Identification of a new low-lying state in the proton drip line nucleus ^{19}Na

C. Angulo,[1] G. Tabacaru,[1,*] M. Couder,[1] M. Gaelens,[1] P. Leleux,[1] A. Ninane,[1] F. Vanderbist,[1] T. Davinson,[2] P. J. Woods,[2] J. S. Schweitzer,[3] N. L. Achouri,[4] J. C. Angélique,[4] E. Berthoumieux,[5] F. de Oliveira Santos,[6] P. Himpe,[7] and P. Descouvemont[8]

[1]*Centre de Recherches du Cyclotron and Institut de Physique Nucléaire, Université Catholique de Louvain, B-1348 Louvain-la-Neuve, Belgium*

[2]*Department of Physics and Astronomy, University of Edinburgh, Edinburgh EH9 3JZ, United Kingdom*

[3]*University of Connecticut, Storrs, Connecticut 06269-3046*

[4]*Laboratoire de Physique Corpusculaire, F-14076 Caen, France*

[5]*DAPNIA/SPhN Bât. 703, CEA, F-91191 Gif sur Yvette Cedex, France*

[6]*GANIL, Bvd. Henri Becquerel, B.P. 5027, F-14076 Caen Cedex 5, France*

[7]*Instituut voor Kern-en Stralingsfysica, Katholieke Universiteit Leuven, B-3001 Leuven, Belgium*

[8]*Physique Nucléaire Théorique et Physique Mathématique CP229, Université Libre de Bruxelles, B-1050 Brussels, Belgium*

(Received 29 July 2002; published 22 January 2003)

The second excited state ($J^\pi = 1/2^+$, $\ell = 0$) of the proton-rich nucleus ^{19}Na has been observed for the first time using the elastic scattering reaction ^{1}H(^{18}Ne,^{1}H)^{18}Ne. An intense (4×10^6 pps) ^{18}Ne radioactive beam was produced at the CRC-RIB facility at Louvain-la-Neuve to bombard a polyethylene target. The recoil protons were detected at 20 different angles in the LEDA segmented silicon detector. The resulting elastic scattering cross sections have been analyzed using a global *R*-matrix fit. We find that the second excited state in ^{19}Na lies at the center-of-mass energy $E_{\text{c.m.}} = 1.066 \pm 0.003$ MeV with respect to the ^{18}Ne$+p$ threshold, and has a proton width $\Gamma_p = 101 \pm 3$ keV. The Coulomb shift between the $1/2^+$ mirror levels in ^{19}O and ^{19}Na is 0.73 MeV, among the largest values currently observed in light exotic nuclei.

DOI: 10.1103/PhysRevC.67.014308 PACS number(s): 27.20.+n, 23.50.+z, 24.30.−v, 25.60.−t

I. INTRODUCTION

The structure of nuclei near the drip lines is one of the major current interests in nuclear physics. Proton-rich light nuclei are a remarkable case since the level scheme is not known for many species. For example, almost no spectroscopic information is available on ^{19}Na, which is proton unbound by 321 ± 13 keV [1]. Even though it is not far from stability, very little is known experimentally about its structure and level scheme: there are no spin assignments, and only the location of the ground state and of the first excited state have been determined by nuclear reactions involving stable beams [2,3]. The ^{19}Na nucleus has also some interest for nuclear astrophysics. The ^{18}Ne$(2p,\gamma)^{20}$Mg reaction may play a role on long-lived waiting point isotopes near the proton drip lines for the *rp*-process reaction flow, although very high densities would be required [4]. However, only the *Q* value of the ^{18}Ne$(p,p)^{18}$Ne reaction is of relevance as the width of its resonances does not enter the reaction rate because production and decay of ^{19}Na are in an equilibrium [5].

The intense low-energy ^{18}Ne radioactive beam at the Louvain-la-Neuve CRC-RIB facility has made possible the study of the low-lying states of ^{19}Na. The aim of the present experiment was to measure the location and the width of the second excited state of ^{19}Na, which according to the mirror nucleus ^{19}O ($E_x = 1.4717 \pm 0.0004$ MeV) should have a spin $J^\pi = 1/2^+$ [1]. The parameters of the ground and the first excited states, whose predicted widths are of the order of eV [1], could not be obtained by the present technique and their measurement was therefore beyond the scope of this work.

The experimental method is described in Sec. II. The data analysis is presented in Sec. III, followed by the conclusions in Sec. IV.

II. EXPERIMENTAL METHOD

We have used the inverse elastic scattering technique by bombarding a proton-rich target with a ^{18}Ne beam at different laboratory energies. The elastic scattering technique has been widely applied in the past for nuclear spectroscopy studies [6–9]. It makes use of the sensitivity of the protons to the presence of a resonant state in the compound nucleus. When the resonant state is scanned with the appropriate ion beam and target, the recoil proton spectra show spectacular changes when detected at forward laboratory angles. These spectra contain precise information on the resonance energy, angular momentum, and width provided all experimental effects, mainly the energy resolution and angular resolution of the detectors, are properly taken into account [10].

Post-accelerated radioactive beams of ^{18}Ne^{2+} at $E_{\text{lab}} = 21$ and 23.5 MeV, and ^{18}Ne^{3+} at $E_{\text{lab}} = 28$ MeV, respectively, were provided by the CYCLONE110 cyclotron. The ^{18}Ne atoms were produced through the ^{19}F$(p,2n)^{18}$Ne reaction by bombarding a LiF target with an intense 30-MeV proton beam produced by the CYCLONE30 cyclotron and were ionized to the 2^+ or to the 3^+ state in a ECR source, before being post-accelerated. A detailed description of the production of the ^{18}Ne radioactive beam can be found in

*Permanent address: NIPNE, P.O. Box MG-6, Magurele-Bucharest, Romania.

Ref. [11]. The average intensity of the ^{18}Ne beams on target was of the order of 4×10^6 pps, which was maintained for periods of several days, allowing us to obtain excellent statistics for each of the three beam energies (the statistical error of the proton events per energy bin of 25 keV at each angle ranges between 1% and 8% for all energies). The target consisted of a 0.5-mg/cm^2 polyethylene $(CH_2)_n$ foil with a very thin Au coating evaporated on the upstream face of the target. We obtained a target thickness of (520 ± 10) μg/cm^2 by measuring the energy loss of the 28-MeV ^{18}Ne beam [12]. The target thickness and the three different beam energies have been chosen such that the energy range of interest could be scanned and the expected interference pattern could clearly show up. A thicker $(CH_2)_n$ target could be used to scan the energy range of interest using a single beam energy. However, the energy straggling of the beam and of the recoil protons would have been larger, introducing an additional uncertainty in the data. The thickness of the Au layer, used for normalization purposes (see below), was obtained by bombarding the targets with a 5.6-MeV ^{7}Li beam. The scattered ^{7}Li on Au and the recoil protons from the ^{1}H(^{7}Li,^{1}H) reaction were detected simultaneously in a PIPS detector located at 60° with respect to the beam axis. The number of Au atoms in the target $N_{\rm Au}$ can be calculated from the relation

$$N_{\rm Au}=N_{\rm p}\frac{C_{\rm p}}{C_{\rm Li}}\frac{(d\sigma/d\Omega)_{\rm Li+p}}{(d\sigma/d\Omega)_{\rm Li+Au}}, \qquad (1)$$

where $N_{\rm p}$ is the number of H atoms in the target, $C_{\rm p}$ and $C_{\rm Li}$ are the number of detected recoil protons and scattered Li, respectively, and $(d\sigma/d\Omega)_{\rm Li+p}$, $(d\sigma/d\Omega)_{\rm Li+Au}$ are the differential cross sections for ^{1}H(^{7}Li,^{1}H)^{7}Li and ^{197}Au(^{7}Li,^{7}Li)^{197}Au, respectively. The ^{1}H(^{7}Li,^{1}H)^{7}Li cross section value was obtained from literature [13]. We have assumed a pure Rutherford cross section for ^{197}Au(^{7}Li,^{7}Li)^{197}Au. We derived a Au layer thickness of 8.0 ± 0.5 μg/cm^2.

The recoil protons were detected in two LEDA segmented silicon detector arrays [14] situated at about 62 and 12 cm from the target. Due to the kinematical variation of the recoil proton energy with laboratory angle, only the 20 most forward angles were used at $\theta_{\rm lab}=4.9°-11.7°$ ($\theta_{\rm c.m}=170.2°-156.6°$) and $\theta_{\rm lab}=22.6°-29.9°$ ($\theta_{\rm c.m}=131.0°-120.2°$), with angular resolution $\Delta\theta_{\rm lab}\simeq0.2°$ and 0.9°, respectively. An 18-μm-thick Mylar foil was situated in front of all LEDA sectors, except one, to stop the high energy scattered ^{18}Ne and most of the recoiled ^{12}C particles, and therefore to reduce the data acquisition dead time. The ''uncovered'' LEDA sector was used for monitoring the number of incoming beam particles by detecting the ^{18}Ne ions scattered on the thin Au layer, assuming a purely Rutherford elastic cross section for ^{197}Au(^{18}Ne,^{18}Ne)^{197}Au at the measured energies. The advantage of this method is that one obtains an intrinsic normalization simultaneously to the recoil proton measurement.

For each LEDA strip, not only the energy but also the time-of-flight (TOF) of the particle with respect to the cyclotron rf were recorded and displayed in a two-dimensional spectrum. Figure 1(a) shows a typical two dimensional spectrum obtained with a 23.5-MeV ^{18}Ne beam on a 0.5-mg/cm^2 polyethylene target during 2 days of running time. The spectrum was obtained by adding the calibrated singles spectra from several LEDA strips at the smallest measured laboratory angle $\theta_{\rm lab}=4.9°$. This spectrum corresponds also to the angle with lowest accumulated statistics (smallest solid angle). The recoil protons, marked by a selection on the figure, are well separated from the recoiled ^{12}C, not completely stopped in the mylar foil, and the uncorrelated β background. In Fig. 1(b), only the proton signal is shown as a function of the proton laboratory energy. The interference pattern between a *s*-wave resonance and the Rutherford contribution is clearly present. Similar spectra were obtained at all measured angles and at beam energies of 21.0, 23.5, and 28.0 MeV, covering laboratory proton energies from 2.1 to 5.5 MeV. Data obtained at overlapping energy regions are in excellent agreement.

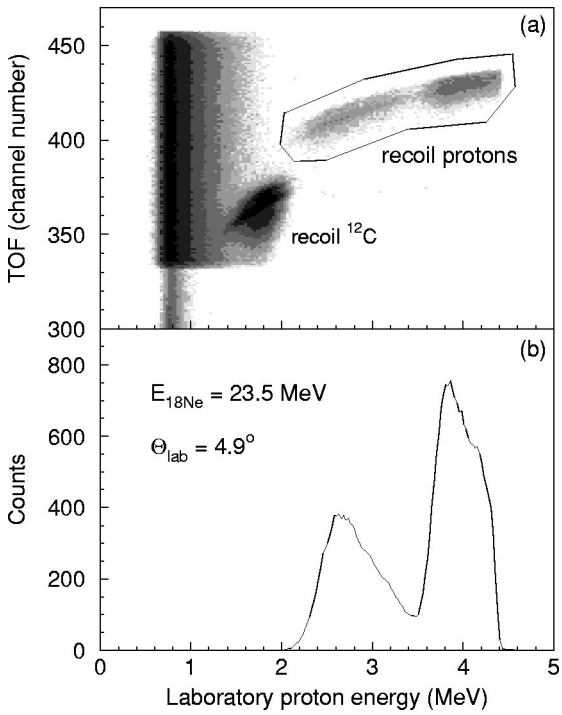

FIG. 1. (a) Summed TOF spectra at $\theta_{\rm lab}=4.9°$ obtained with a 23.5-MeV ^{18}Ne beam on a ''nominal'' 0.5-mg/cm^2 polyethylene target. The recoil protons are marked by a selection on the figure. (b) The proton signal is shown as a function of the proton laboratory energy.

III. DATA ANALYSIS AND DISCUSSION

In reverse kinematics, the c.m. energy $E_{\rm c.m.}$ is related to the laboratory energy of the protons $E_{\rm p}$, recoiling at the laboratory angle $\theta_{\rm lab}$ by

$$E_{\rm c.m.}=E_{\rm p}\times\frac{M_{\rm b}+1}{4M_{\rm b}\cos^2\theta_{\rm lab}}, \qquad (2)$$

where $M_{\rm b}$ is the mass number of the beam. The tranformation of the scattering angle and the differential cross section to the c.m. frame is given by

$$\theta_{\text{c.m.}} = \pi - 2\,\theta_{\text{lab}} \tag{3}$$

and

$$\frac{d\sigma}{d\Omega_{\text{c.m}}}(E_{\text{c.m}}, \theta_{\text{c.m.}}) = \frac{d\sigma}{d\Omega_{\text{lab}}}(E_{\text{lab}}, \theta_{\text{lab}})/4\cos\theta_{\text{lab}}. \tag{4}$$

The proton spectra are slightly degraded by two experimental effects: (i) the opening angle of the detectors ($\Delta\theta_{\text{lab}}$), introducing an uncertainty in the proton energy ΔE_θ, given by [7]

$$\Delta E_\theta = 2E_{\text{p}} \tan\theta_{\text{lab}} \Delta\theta_{\text{lab}}, \tag{5}$$

and (ii) the energy straggling of the protons ΔE_{strag} in the target and in the mylar foil used to stop the heavier ions. A good estimate of ΔE_{strag} is obtained by using the Bohr formula [15]. The total energy broadening (ΔE) is obtained by adding quadratically ΔE_θ and ΔE_{strag}. Typical values of ΔE are 12 keV for a laboratory angle of $\theta_{\text{lab}} = 4.9°$, 17 keV for $\theta_{\text{lab}} = 11.7°$ (ΔE_{strag} is the most important contribution in both cases), and 40 keV for $\theta_{\text{lab}} = 29.9°$ (ΔE_θ is the most important contribution).

From the recoil proton spectra we have obtained differential cross sections, for each of the 20 laboratory angles and for c.m. energies in the range $E_{\text{c.m.}} = 0.7$–1.5 MeV, by correcting the number of counts for the solid angle of the detectors, the number of protons in the target, and the total number of incident beam particles (obtained by the normalization on Au, as explained above). Corrections for energy loss in the target and in the mylar foil have also been applied [12]. Figure 2 shows the differential cross section versus c.m. energies for three typical c.m. angles (a) 170.2°, (b) 156.6°, and (c) 120.2°. The total error includes the statistical error and the uncertainties due to the normalization and the energy calibration. The dotted curve is the Rutherford cross section.

We have used the *R*-matrix formalism [16] to fit the differential cross sections in the 120.2°–170.2° angular range and the 0.7–1.5-MeV c.m. energy range. In the *R*-matrix theory, the nuclear phase shift is defined by

$$\delta^\ell = \delta^\ell_{\text{HS}} + \delta^\ell_{\text{R}}, \tag{6}$$

where δ^ℓ_{HS} and δ^ℓ_{R} are the hard-sphere and the *R*-matrix phase shifts, respectively. Here, we have used hard-sphere phase shifts for all partial waves (ℓ values up to $\ell_{\text{max}} = 2$ have been taken into account) except for $\ell = 0$, where we have applied the *R*-matrix phase shift given by

$$\delta^0_{\text{R}} = \arctan\frac{P_0 R^0}{1 - S_0 R^0}, \tag{7}$$

where P_0 and S_0 are the $\ell = 0$ penetration and shift factors, respectively, and R^0 is the *R*-matrix defined with a single pole. The fitted parameters are the pole parameters converted to the resonance energy E_{R} and the proton width Γ_{p} of the $1/2^+$ state in ^{19}Na (in *R*-matrix notation, E_{R} and Γ_{p} are "observed" parameters). In order to account for the experimental effects described above, we have convoluted the calculations with a Gaussian distribution, with a full width at half maximum ΔE, which was set equal to the total energy broadening as calculated above.

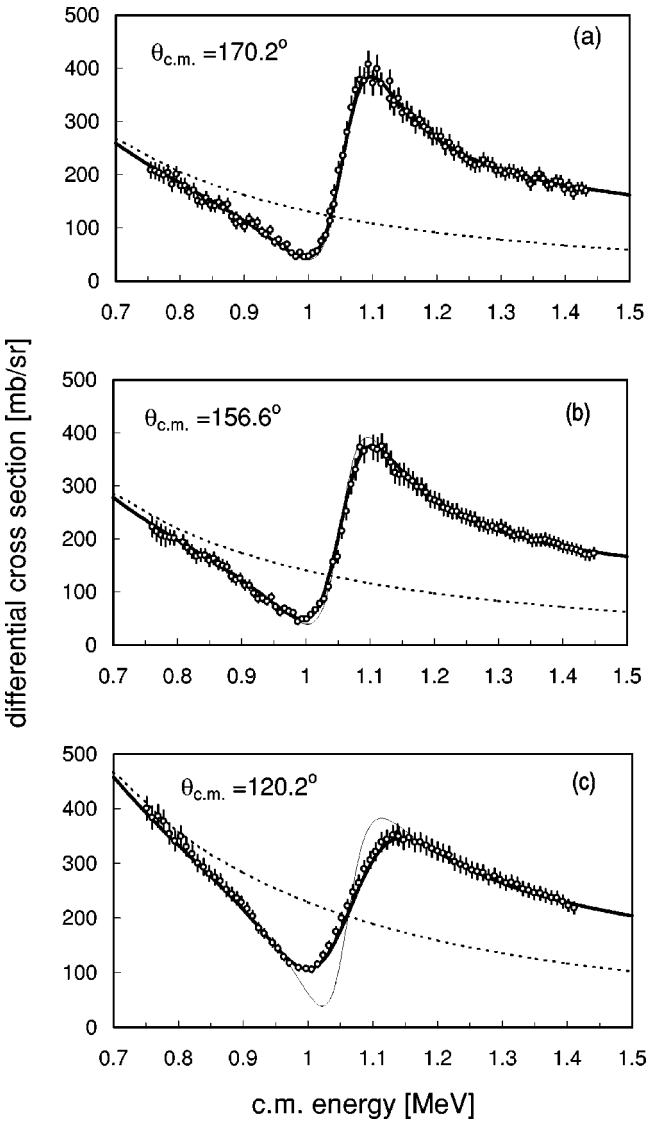

FIG. 2. Elastic cross section versus c.m. energies for the system ^{18}Ne+p for c.m. angles (a) 170.2°, (b) 156.6°, and (c) 120.2°. The thicker solid curves are *R*-matrix fits ($a = 5$ fm) with parameters of Table I, that includes an energy correction for opening angle and beam straggling. The thinner solid curve are the fits obtained without ΔE folding. The dotted curves are the Rutherford cross sections.

We have tested the sensitivity of the fit to the *R*-matrix channel radius a by performing global fits for three different values $a = 4$,5, and 6 fm. The results of these fits are presented in Table I. The quoted errors include an uncertainty of 3 keV due to the data bining. We have adopted the values for $a = 5$ fm, which provides the lowest χ^2/N value, $\chi^2/N = 0.44$ for $E_{\text{R}} = 1.066 \pm 0.003$ MeV and $\Gamma_{\text{p}} = 101 \pm 3$ keV. The small errors are due to the strong sensitivity of χ^2 with respect to E_{R} and Γ_{p}. The thicker solid curve in Fig. 2 is the *R*-matrix fit ($a = 5$ fm) for the adopted values (Table I) and includes the correction for opening angle and beam strag-

TABLE I. Results of the *R*-matrix fits ($N=367$).

	$a=4$ fm	$a=5$ fm	$a=6$ fm
E_R (MeV)	1.067 ± 0.003	1.066 ± 0.003	1.064 ± 0.003
Γ_p (keV)	104 ± 3	101 ± 3	95 ± 3
χ^2/N	0.53	0.44	0.49
θ_p^2 (%)	29.8	22.9	21.6

gling discussed above. The thinner solid curve [unresolved for (a)] corresponds to $\Delta E=0$. *R*-matrix fits using other spin assignments strongly disagree with the experimental data. The dimensionless reduced width θ_p^2 represents more than 20% of the Wigner limit. This value is similar to or even larger than the reduced width of $\ell=0$ states in other nuclei such as ^{13}N ($E_x=2.37$ MeV, $\theta_p^2=21.8\%$) or ^{14}O ($E_x=5.17$ MeV, $\theta_p^2=21.4\%$).

The isobar diagram for the mirror nuclei ^{19}O and ^{19}Na is shown in Fig. 3, including the new $1/2^+$ state in ^{19}Na. The large θ_p^2 value is also consistent with the important Coulomb shift (shown by an arrow in the figure). In ^{19}O, the excitation energy of the mirror state is $E_x=1.472$ MeV [1] whereas it is $E_x=0.745\pm0.013$ MeV for ^{19}Na. This Coulomb shift ($\sim$0.73 MeV) is among the largest values observed in light nuclei. It is typical of deformed states, found in nuclei near the drip lines.

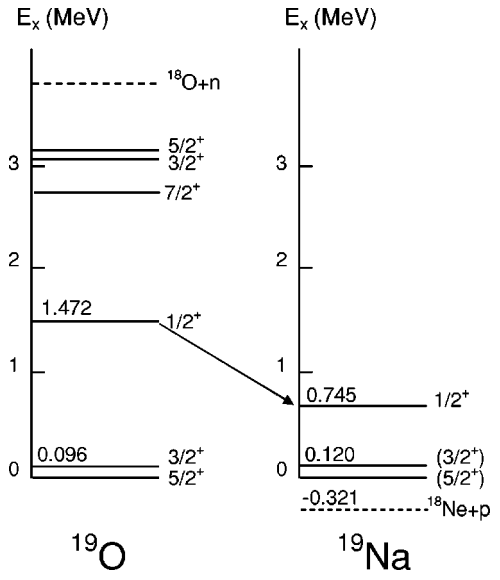

FIG. 3. Isobar diagram for ^{19}O and ^{19}Na.

IV. CONCLUSIONS

Using a low-energy ^{18}Ne radioactive beam and a thin polyethylene target we have measured the elastic scattering reaction ^{1}H(^{18}Ne,^{1}H)^{18}Ne. From a global *R*-matrix fit for c.m. energies $E_{c.m.}=0.7$–1.5 MeV and c.m. angles $\theta_{c.m}=120.2°$–$170.2°$, we have determined the energy and the width of the $1/2^+$ state in ^{19}Na, $E_R=1.066\pm0.003$ MeV and $\Gamma_p=101\pm3$ keV. This state corresponds to the mirror of the $E_x=1.472$ MeV state in ^{19}O. We find a very large reduced width, typical of deformed states. Consequently the Coulomb shift of this state with respect to the mirror one in ^{19}O is among the largest values observed in light nuclei.

According to the mirror nucleus ^{19}O, several states should be present in the c.m. energy range 2–3 MeV. In order to obtain a global picture of the low-energy states of ^{19}Na, further investigations are planned in the near future.

ACKNOWLEDGMENTS

We thank the CRC staff for their dedication to the production of the ^{18}Ne beam and the technical support during the experiment. We also thank P. Demaret for the skillful target preparation and J. Cabrera for help on the data analysis. This work has been supported by the European Community-Access to Research Infrastructure Action of the Improving Human Potential Program, Contract No. HPRICT199900110 and the Belgian Program P5/07 on Interuniversity Attraction Poles of the Belgian-state Federal Services for Scientific, Technical and Cultural Affairs. M.G., P.D., and P.L. acknowledge the support of the National Fund for Scientific Research (FNRS), Belgium. T.D. and P.J.W. acknowledge the support of the Engineering and Physical Sciences Research Council (EPSRC), UK.

[1] D. R. Tilley *et al.*, Nucl. Phys. **A595**, 1 (1995).
[2] J. Cerny *et al.*, Phys. Rev. Lett. **22**, 612 (1969).
[3] W. Benenson *et al.*, Phys. Lett. **58B**, 46 (1975).
[4] J. Görres *et al.*, Phys. Rev. C **51**, 392 (1995).
[5] J. Görres (private communication).
[6] P. Decrock *et al.*, Phys. Rev. Lett. **67**, 808 (1991).
[7] R. Coszach *et al.*, Phys. Lett. B **353**, 184 (1995).
[8] D. W. Bardayan *et al.*, Phys. Rev. Lett. **83**, 45 (1999).
[9] J.-S. Graulich *et al.*, Phys. Rev. C **63**, 011302(R) (2000).
[10] J.-S. Graulich *et al.*, Eur. Phys. J. A **13**, 221 (2002).
[11] M. Gaelens *et al.*, Proceedings of the 15th International Conference on Application of Accelerators in Research and Industry, Denton, 1998, ISBN-1-56396-825-8, p. 305.
[12] J. F. Ziegler and J. P. Biersack, SRIM2000 program, version 39, 1998, 1999, IBM Co.
[13] W. D. Warters *et al.*, Phys. Rev. **91**, 917 (1953).
[14] T. Davinson *et al.*, Nucl. Instrum. Methods Phys. Res. A **454**, 350 (2000).
[15] N. Bohr, K. Dan. Vidensk. Selsk. Mat. Fys. Medd. **18**, 8 (1948).
[16] A. M. Lane and R. G. Thomas, Rev. Mod. Phys. **30**, 257 (1958).